ELSEVIER

Journal of Molecular Catalysis A: Chemical 171 (2001) 217–227

JOURNAL OF MOLECULAR CATALYSIS A: CHEMICAL

www.elsevier.com/locate/molcata

Halo-oxide $ACuO_{2-\delta}X_{\sigma}$ ($A = Sr_{0.63}Ca_{0.27}$, X = F, Cl) catalysts active and durable for ethane selective oxidation to ethene

H.X. Dai [a,b], H. He [a,c], C.F. Ng [a], C.T. Au [a,*]

[a] *Department of Chemistry, Hong Kong Baptist University, Kowloon Tong, Kowloon, Hong Kong, PR China*
[b] *Department of Applied Chemistry, Faculty of Science, Beijing University of Chemical Technology, Beijing 100029, PR China*
[c] *College of Environmental and Energy Engineering, Beijing Polytechnic University, Beijing 100022, PR China*

Received 11 September 2000; accepted 24 January 2001

Abstract

The catalytic performance and characterization of $ACuO_{2-\delta}$ ($A = Sr_{0.63}Ca_{0.27}$) and $ACuO_{2-\delta}X_{\sigma}$ (X = F, Cl) catalysts have been investigated for the oxidative dehydrogenation of ethane (ODE) to ethene. The results of X-ray diffraction indicated that the three catalysts are single-phase and tetragonal infinite-layer in structure. The incorporation of fluoride or chloride ions in the $ACuO_{2-\delta}$ lattice can significantly enhance C_2H_6 conversion and C_2H_4 selectivity. At $C_2H_6/O_2/N_2$ molar ratio = 2/1/3.7 and space velocity = 6000 ml h^{-1} g^{-1}, we observed 73.5% C_2H_6 conversion, 67.2% C_2H_4 selectivity, and 49.4% C_2H_4 yield at 660°C over $ACuO_{1.901}F_{0.088}$, and 87.4% C_2H_6 conversion, 74.4% C_2H_4 selectivity, and 65.0% C_2H_4 yield at 680°C over $ACuO_{1.950}Cl_{0.036}$. With the decrease in C_2H_6/O_2 molar ratio, C_2H_6 conversion increased, whereas C_2H_4 selectivity decreased. Within 48 h of on-stream ODE reaction, the two halide-doped materials exhibited sustainable catalytic performance. Based on the results of X-ray photoelectron spectroscopy, O_2 temperature-programmed desorption, and C_2H_6 and $C_2H_6/O_2/N_2$ (2/1/3.7 molar ratio) pulse studies, we conclude that (i) the incorporation of halide ions into the $ACuO_{2-\delta}$ lattice could enhance lattice oxygen activity, and (ii) in excessive amount, the O^- species accommodated in oxygen vacancies and desorbed below 600°C tend to induce ethane complete oxidation, whereas the lattice oxygen species desorbed above 600°C are active for ethane selective oxidation to ethene. By regulating the oxygen vacancy density and Cu^{3+} population in the halo-oxide catalyst, one can generate a durable catalyst with good performance for the ODE reaction.

Keywords: Ethane oxidative dehydrogenation to ethene; ODE reaction; Infinite-layer halo-oxide catalyst; $(Sr_{0.63}Ca_{0.27})CuO_{2-\delta}X_{\sigma}$ (X = F, Cl); XPS characterization; Superconducting cuprate material

1. Introduction

In the past decades, the oxidative dehydrogenation of ethane (ODE) to ethene has been investigated intensively and extensively. Many compounds have been tested as catalysts for this reaction. Among them, $Li^+-MgO-Cl^-$ seems to be the most effective (ca. 58% C_2H_4 yield at 620°C) [1]. Although $KSr_2Bi_3O_4Cl_6$ [2], a layered complex compound, gave ca. 70% C_2H_4 yield at 640°C, the catalyst deteriorated due to Cl leaching. Recently, Takehira et al. [3] investigated a series of $La_{1-x}Sr_xFeO_{3-\delta}$ catalysts for the ODE reaction and found that $SrFeO_{3-\delta}$ showed the best catalytic performance (87% C_2H_6 conversion, 43% C_2H_4 selectivity, and 37% C_2H_4 yield at 650°C). Such a catalytic activity was believed to be associated with the density of oxygen vacancies and the concentration of hypervalent iron cations.

* Corresponding author. Tel.: +852-2339-7067; fax: +852-2339-7348.
E-mail address: pctau@hkbu.edu.hk (C.T. Au).

1381-1169/01/$ – see front matter
PII: S1381-1169(01)00105-4

Composite oxides such as perovskite-type and perovskite-like oxides are known to be active for the total oxidation of CO and HC (hydrocarbons) [4,5]. The high oxygen vacancy density and strong redox ability of these catalysts play important roles in catalyzing the complete oxidation reactions. Generally speaking, the higher oxygen vacancy density and the stronger the redox ability, the better the composite oxide catalyst performs. If one could decrease the oxygen vacancy density and increase the redox ability by incorporating halide ions (with ionic radii similar to O^{2-} ions) to the vacant oxygen positions, it is possible to convert these combustion materials to catalysts selective for the oxidation of ethane to ethene. Based on this idea, we generated several classes of halide-doped composite oxide catalysts. In our previous studies, we have characterized and reported $SrFeO_{3-\delta}Cl_\sigma$ [6], $La_{1-x}Sr_xFeO_{3-\delta}X_\sigma$ (X = F, Cl) [7] $YBa_2Cu_3O_{7-\delta}X_\sigma$ (X = F, Cl) [8], and hole-doped $La_{1.85}Sr_{0.15}CuO_{4-\delta}X_\sigma$ (X = F, Cl) and electron-doped $Nd_{1.85}Ce_{0.15}CuO_{4-\delta}X_\sigma$ catalyst [9], which showed good activity and durability for the ODE reaction. The above series of composite oxides exhibit an anionic defect character. To further our investigation, we turned our attention to $ACuO_{2-\delta}$ ($A = Sr_{0.63}Ca_{0.27}$). In the structure of this p-type superconducting material that shows a transition temperature (T_c) of up to 110 K, there are both cationic and anionic defects [10]. In this study, we report the catalytic performance and characterization of $ACuO_{2-\delta}X_\sigma$ (X = F, Cl) as well as $ACuO_{2-\delta}$ (for comparison purposes) for the partial oxidation of ethane to ethene.

2. Experimental

The $ACuO_{2-\delta}$ catalyst was prepared according to the method described by Azuma et al. [10]. Stoichiometric amounts of $Sr(NO_3)_2$, $Ca(NO_3)_3{\cdot}4H_2O$, and $Cu(NO_3)_2{\cdot}6H_2O$ (Aldrich, >99.9%) were mixed and calcined at 960°C for a total of 47 h with two intermediate grinding. The fluorination or chlorination of $ACuO_{2-\delta}$ was carried out in a vacuum (ca. 0.1 Torr) furnace first at 350°C for 10 h and then at 660°C for 15 h by using NH_4F or NH_4Cl as halogenating reagent [11]. After halogenation, the samples were quenched to room temperature and were in turn ground, tableted, crushed, and sieved to a size range of 80–100 mesh.

Catalytic activity was tested at 1 atm with 0.5 g of the catalyst in a fixed-bed quartz micro-reactor (i.d. = 4 mm); the reaction temperatures were from 520 to 680°C at 20°C intervals. A mixture of ethane (14.8 ml min^{-1}) and air (35.2 ml min^{-1}) was passed through the reactor, corresponding to a contact time of 1.67×10^{-4} h g ml^{-1} and a $C_2H_6/O_2/N_2$ molar ratio of 2/1/3.7. The product mixture (C_2H_6, C_2H_4, CH_4, CO, and CO_2) was analyzed on-line by gas chromatograph (Shimadzu 8A TCD) with Porapak Q and 5A Molecular Sieve columns. In a blank experiment, quartz sand showed 5.0% C_2H_6 conversion, 88.0% C_2H_4 selectivity, and 4.4% C_2H_4 yield at 680°C, indicating that homogeneous reaction is insignificant at or below 680°C. We observed that further rise in temperature would result in substantial gas-phase reaction. Therefore, the catalytic performances of these materials were examined only at or below 680°C. For the variation of $C_2H_6/O_2/N_2$ molar ratio, the flow rates of C_2H_6, O_2, and N_2 were varied at a fixed contact time (1.67×10^{-4} h g ml^{-1}).

The crystal structures of the catalysts were determined by an X-ray diffractometer (XRD, D-MAX, Rigaku) operating at 40 kV and 200 mA using Cu Kα radiation. X-ray photoelectron spectroscopic (XPS, Leybold Heraeus, VG CLAM 4 MCD Analyzer) technique with Mg Kα ($h\nu = 1253.6$ eV) being the excitation source was used to determine the Cu $2p_{3/2}$ and O 1s binding energies of surface copper and oxygen species, respectively. The instrumental resolution was 0.5 eV. Before XPS measurements, the samples were calcined in O_2 (flow rate, 20 ml min^{-1}) at 850°C for 1 h and then cooled in O_2 to room temperature, followed by treatments in He (20 ml min^{-1}) at a desired temperature for 1 h and then cooled in He to room temperature. Finally, the samples were outgassed in the primary vacuum chamber (10^{-5} Torr) for 0.5 h and then introduced into the ultrahigh vacuum chamber for recording. The C 1s line at 284.6 eV was taken as a reference for binding energy calibration. The specific surface areas of the catalysts were measured using a Nova 1200 apparatus.

The O_2-TPD (temperature-programmed desorption) experiments were performed according to the methods described in [12]. The temperature range was from room temperature to 950°C and the heating rate was

$10^{\circ}C\,min^{-1}$. The amount of O_2 desorbed from the catalysts was quantified by calibrating the peak areas against that of a standard pulse.

We performed pulse experiments to investigate the reactivity of surface oxygen species. A catalyst sample (0.2 g) was placed in a micro-reactor and was thermally treated at a desired temperature for 30 min before the pulsing of C_2H_6 or $C_2H_6/O_2/N_2$ (2/1/3.7 molar ratio), and the effluent was analyzed on-line by a mass spectrometer (HP G1800A). The pulse size was 65.7 μl (at 25°C, 1 atm) and He (HKO Co., >99.995%) was the carrier gas.

The contents of halogen and Cu^{3+} or Cu^{+} were determined by adopting the methods previously described [8,13]. The experimental errors are ±0.05% for halide analysis and ±0.5% for Cu^{3+} and Cu^{+} titrations.

3. Results and discussion

3.1. Catalyst compositions, surface areas, structures, and catalytic performance

Table 1 shows the structures, compositions, and surface areas of $ACuO_{2-\delta}$ and $ACuO_{2-\delta}X_{\sigma}$. According to the Cu^{3+} and halogen contents as well as with the assumption of preserving electroneutrality, the value of δ was calculated to be 0.074 for $ACuO_{2-\delta}$, whereas the values of δ and σ were estimated to be 0.099 and 0.088 for $ACuO_{2-\delta}F_{\sigma}$, 0.050 and 0.036 for $ACuO_{2-\delta}Cl_{\sigma}$, respectively. The amount of nonstoichiometric oxygen was 0.074 for $ACuO_{1.926}$, 0.011 for $ACuO_{1.901}F_{0.088}$, and 0.014 for $ACuO_{1.950}Cl_{0.036}$. From Table 1, one can observe that the inclusion of halide ions in $ACuO_{2-\delta}$ induced a rise in Cu^{3+} content and a decrease in oxygen vacancy density with no significant decline in surface area; there were also no significant changes in F or Cl content of the halogenated catalyst before and after 48 h of on-stream reaction. Fig. 1 shows the XRD patterns of $ACuO_{1.926}$ and $ACuO_{2-\delta}X_{\sigma}$. Besides a trace amount of the $(Sr, Ca)_{14}Cu_{24}O_{41}$ phase, the three catalysts could be considered as single-phase and are tetragonal infinite-layer in structure (as indexed in Fig. 1b and c), in good agreement with those reported in the literature [10,14,15]. The similarity in crystal structure of the undoped (Fig. 1a) and halide-doped (Fig. 1b and c) materials indicates that the halide ions were incorporated into the $ACuO_{2-\delta}$ lattice.

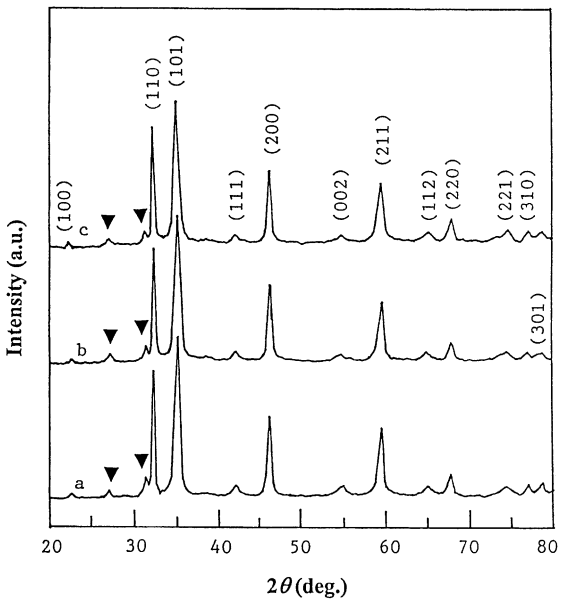

Fig. 1. XRD patterns of (a) $ACuO_{1.926}$, (b) $ACuO_{1.901}F_{0.088}$, and (c) $ACuO_{1.950}Cl_{0.036}$. Tetragonal phase was indexed and symbol (▼) denotes the $(Sr, Ca)_{14}Cu_{24}O_{41}$ phase.

Fig. 2 shows the catalytic performance of $ACuO_{1.926}$ and $ACuO_{2-\delta}X_{\sigma}$ (X = F, Cl) after 1 h of on-stream ODE reaction. Over the undoped catalyst (Fig. 2a), with the rise in reaction temperature, the C_2H_6 conversion, O_2 conversion, C_2H_4 selectivity, C_2H_4

Table 1
Chemical compositions and surface areas of $ACuO_{2-\delta}$ and $ACuO_{2-\delta}X_{\sigma}$ (X = F, Cl) catalysts

Catalyst	Cu^{3+} content (mol%)	X content (wt.%)	δ	σ	Surface area ($m^2\,g^{-1}$)
$ACuO_{2-\delta}$	5.2	–	0.074	–	3.0
$ACuO_{2-\delta}F_{\sigma}$	9.1	1.06 (1.04)[a]	0.099	0.088	2.7
$ACuO_{2-\delta}Cl_{\sigma}$	13.6	0.81 (0.82)[a]	0.050	0.036	2.6

[a] After 48 h of on-stream reaction.

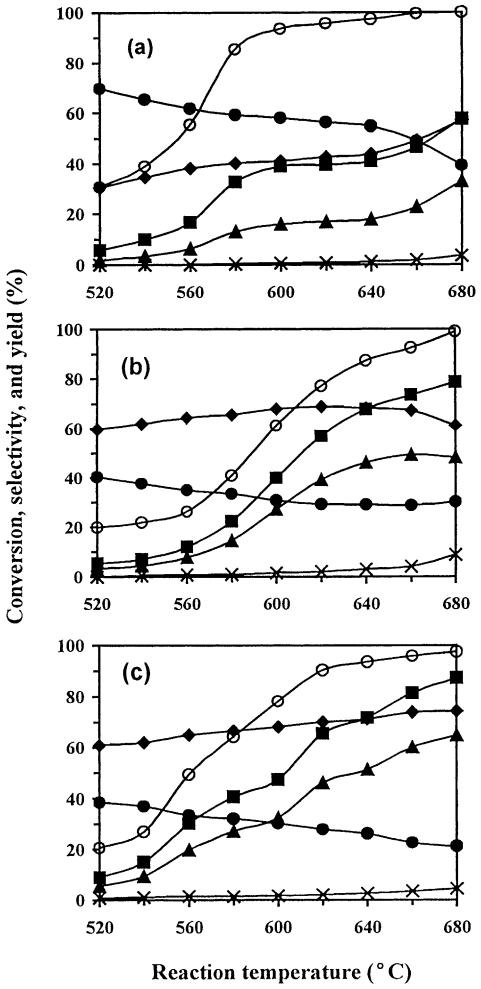

Fig. 2. Catalytic performance of (a) $ACuO_{1.926}$, (b) $ACuO_{1.901}F_{0.088}$, and (c) $ACuO_{1.950}Cl_{0.036}$ as related to reaction temperature. (■) C_2H_6 conversion; (◆) C_2H_4 selectivity; (▲) C_2H_4 yield; (×) CH_4 selectivity; (●) CO_x selectivity; (○) O_2 conversion.

yield, and CH_4 selectivity increased, whereas CO_x (i.e. CO + CO_2) selectivity decreased. Over the $ACuO_{1.901}F_{0.088}$ catalyst (Fig. 2b), when the temperature was raised from 520 to 680°C, C_2H_6 and O_2 conversions and CH_4 selectivity increased, and C_2H_4 selectivity and C_2H_4 yield first increased and then decreased, reaching a maximal value of 68.8% (at 620°C) and 49.4% (at 660°C), respectively, whereas CO_x selectivity first decreased and then increased, reaching a minimal value of 28.7% at 660°C. Over the $ACuO_{1.950}Cl_{0.036}$ catalyst (Fig. 2c), similar trends were observed: with the rise in temperature, C_2H_6 and O_2 conversions, and CH_4 selectivity augmented, the maximal C_2H_4 selectivity (74.4%) and C_2H_4 yield (65.0%) appeared at 680°C where CO_x selectivity reached a minimal value of 21.1%. Similar results were obtained when each of the two halo-oxide catalysts was well dispersed in quartz sand (0.5 g catalyst per 5.0 g quartz sand). This indicates that the problem of hot spots was insignificant. The formation of CH_4 requires the breakage of C–C bond. Kennedy and Cant [16] proposed that CH_4 could be generated via (i) C_2H_6 decomposition in the gas phase and (ii) a heterogeneous pathway involving an ethylperoxy intermediate. In the latter case, ethylperoxy reacted with surface oxygen species to form CH_4 and HCO_2, and the HCO_2 species were further oxidized to CO_x and H_2O. Based on these results, one can conclude that the $ACuO_{2-\delta}X_\sigma$ catalysts are much superior to the $ACuO_{1.926}$ catalyst in catalyzing the ODE reaction.

In the lifetime studies, we examined the catalytic performance of $ACuO_{1.901}F_{0.088}$ and $ACuO_{1.950}Cl_{0.036}$ in 48 h of on-stream reaction. It is observed that both catalysts displayed stable behaviors (Fig. 3). As shown in Table 1, the F or Cl contents of the fresh and used (after 48 h of reaction) halide-incorporated catalysts were rather similar, implying that the $ACuO_{2-\delta}X_\sigma$ catalysts were rather intact after 48 h.

In the studies of the effects of $C_2H_6/O_2/N_2$ molar ratio on the catalytic performance of $ACuO_{1.901}F_{0.088}$ (at 660°C) and $ACuO_{1.950}Cl_{0.036}$ (at 680°C), we observed that with the variation of $C_2H_6/O_2/N_2$ molar ratio from 1/2/3.7 to 2/1/3.7, C_2H_6 conversion and CO_x selectivity decreased from 75.8 and 33.2% to 73.5 and 28.7% over the F-doped catalyst, and from 89.9 and 27.2% to 87.4 and 21.1% over the Cl-doped catalyst, respectively, whereas O_2 conversion, C_2H_4 selectivity, and C_2H_4 yield increased from 27.6, 64.1, and 48.6% to 92.5, 67.2, and 49.4% over the former catalyst and from 29.9, 69.8, and 62.8% to 97.4, 74.4, and 65.0% over the latter catalyst, respectively.

In order to investigate the reactivity of C_2H_4 towards O_2 over the three catalysts, we carried out C_2H_4 oxidation experiments under reaction conditions similar to those in the C_2H_6 oxidation reaction, and the results are listed in Table 2. One can observe that the C_2H_4 conversion was 18.4% over the F-doped catalyst and 14.2% over the Cl-doped catalyst, whereas

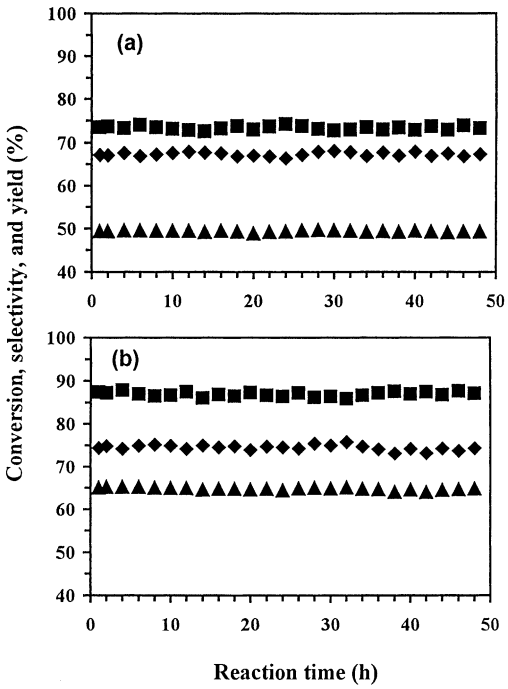

Fig. 3. Catalytic performance of (a) $ACuO_{1.901}F_{0.088}$ at 660°C and (b) $ACuO_{1.950}Cl_{0.036}$ at 680°C as a function of reaction time. (■) C_2H_6 conversion; (◆) C_2H_4 selectivity; (▲) C_2H_4 yield.

over $ACuO_{1.926}$, it was 32.6%. Furthermore, the CO/CO_2 ratios in the product mixture observed over $ACuO_{2-\delta}X_\sigma$ were much higher than that observed over $ACuO_{1.926}$. Lunsford et al. [17] pointed out that C_2H_4 was the major carbon source for CO_x formation at or above 650°C. As revealed in the studies of the effects of $C_2H_6/O_2/N_2$ molar ratio on the ODE performance, the two halide-doped catalysts exhibited the same variation trend in reactant conversions and product selectivities with the change in $C_2H_6/O_2/N_2$ molar ratio; the rise of O_2 concentration in the feedstock caused an increase in C_2H_6 conversion but a decrease in C_2H_4 selectivity. The C_2H_6/O_2 molar ratio required for the selective oxidation of C_2H_6 to C_2H_4 is 2/1. An excessive amount of O_2 would be unfavorable for the ODE reaction at high temperatures (>660°C). The increase in selectivity towards one of the products with the increase in reactant conversion is unusual in heterogeneous catalysis. However, if the C_2H_4 deep oxidation was reduced or suppressed, C_2H_4 selectivity would be enhanced. In C_2H_6 oxidation at a particular O_2 conversion, the simultaneous augmentation in C_2H_4 selectivity and C_2H_6 conversion is due to a reduction in C_2H_4 deep oxidation (Table 2).

3.2. Copper oxidation state, oxygen vacancy density, and halide location

In the ideal crystal structure of $Sr_{1-x}Ca_xCuO_2$, there are no cationic and anionic defects and the oxidation state of Cu is 2+. On the ground of preserving electroneutrality, the existence of cationic defects would give rise to the rise in Cu oxidation state (which favors the redox process of the catalyst [18]) and/or the formation of oxygen vacancies (which favors the deep oxidation of HC [4,5]). Theoretically, the halide ions incorporated into the $ACuO_{2-\delta}$ lattice could (i) replace some of the O^{2-} ions, (ii) occupy oxygen vacancies, or (iii) dwell at interstitial sites. If a F^- or Cl^- ion replaces an O^{2-} ion, to maintain electroneutrality, the oxidation state of an adjacent copper ion has to drop; if a halide ion occupies an oxygen vacancy or an interstitial position, it would cause the oxidation state of an adjacent copper ion to rise. As a matter of fact, the introduction of F^- or Cl^- ions into $ACuO_{2-\delta}$ caused the Cu^{3+} contents to increase rather than to decrease (Table 1), demonstrating that

Table 2
Catalytic performance of $ACuO_{1.926}$ at 680°C, $ACuO_{1.901}F_{0.088}$ at 660°C, and $ACuO_{1.950}Cl_{0.036}$ at 680°C for the oxidation of ethane and ethene at 6000 ml h^{-1} g^{-1}

Catalyst	Oxidation of C_2H_4[a]		Oxidation of C_2H_6	
	C_2H_4 conversion (%)	CO/CO_2 ratio	C_2H_6 conversion (%)	C_2H_4 selectivity (%)
$ACuO_{1.926}$	32.6	1/19.6	57.6	57.1
$ACuO_{1.901}F_{0.088}$	18.4	1/6.4	73.5	67.2
$ACuO_{1.950}Cl_{0.036}$	14.2	1/4.5	87.4	74.4

[a] At $C_2H_4/O_2/N_2$ molar ratio = 2/1/3.7.

Table 3
Changes of Cu^{3+} contents in $ACuO_{1.926}$, $ACuO_{1.901}F_{0.088}$, and $ACuO_{1.950}Cl_{0.036}$ after thermal treatments in He at 520, 580, and 680°C, respectively[a]

Catalyst	Cu^{3+} content (mol%)			Halide content at 800°C[b] (wt.%)
	520°C	580°C	680°C	
$ACuO_{1.926}$	2.8 (5.3)	1.2 (5.1)	0.9 (5.4)	–
$ACuO_{1.901}F_{0.088}$	8.3 (8.9)	7.8 (9.2)	3.2 (9.1)	1.02
$ACuO_{1.950}Cl_{0.036}$	12.6 (13.7)	11.7 (13.5)	4.4 (13.8)	0.80

[a] Values in parentheses were obtained after the thermally treated sample was exposed to an oxygen flow of 20 ml min^{-1} at the same temperature for 30 min.
[b] Halide contents of the samples thermally treated in He at 800°C for 30 min.

the halide ions have occupied a certain amount of oxygen vacancies and/or interstitial spacings [19,20].

Summarized in Table 3 are the changes of Cu^{3+} contents in $ACuO_{1.926}$, $ACuO_{1.901}F_{0.088}$, and $ACuO_{1.950}Cl_{0.036}$ under various thermal treatments. With a rise in temperature from 520 to 680°C in a He atmosphere, the Cu^{3+} content decreased significantly. It indicates that the abatement in Cu^{3+} content is induced by the desorption of oxygen species on/in the catalysts. Exposing the treated samples to an oxygen flow at the same temperature for 30 min restored the Cu^{3+} contents to their former values (Table 1), indicating that the Cu^{3+} amounts could be replenished via the oxidation of Cu^{2+}. There was no significant change in halide content when the catalysts were heated in He at 800°C for 30 min. These results indicate that in an oxygen-deprived atmosphere, the drop in Cu^{3+} content is due to the desorption of oxygen species.

Fig. 4 shows the Cu $2p_{3/2}$ spectra of the $ACuO_{1.926}$ and $ACuO_{2-\delta}X_{\sigma}$ samples which had been treated in He at 520, 580, and 680°C, respectively. It is observed that the intensities of the shake-up satellite signals increased with the rise in treatment temperature, possibly associated with the increase in Cu^{2+} concentration due to the desorption of oxygen at elevated temperatures. The shake-up satellites observed in the Cu $2p_{3/2}$ spectra (Fig. 4) were caused by the charge transferred from neighboring oxygen ligands into an empty d-state of Cu^{2+} ion [21]. The Cu $2p_{3/2}$ binding energy was at ca. 933.5 eV for the halogen-free and halogen-containing catalysts. Since the binding energy of the 2p electrons of Cu^{3+} is larger than that of Cu^{2+} (ca. 933.5 eV) or Cu^{+} (ca. 932.7 eV) [22], the peak corresponding to Cu^{3+} is expected to appear at a higher binding energy. From Fig. 4, one can observe a shoulder peak at ca. 935.0 eV, denoting the presence of Cu^{3+} in these catalysts; furthermore, the signal of

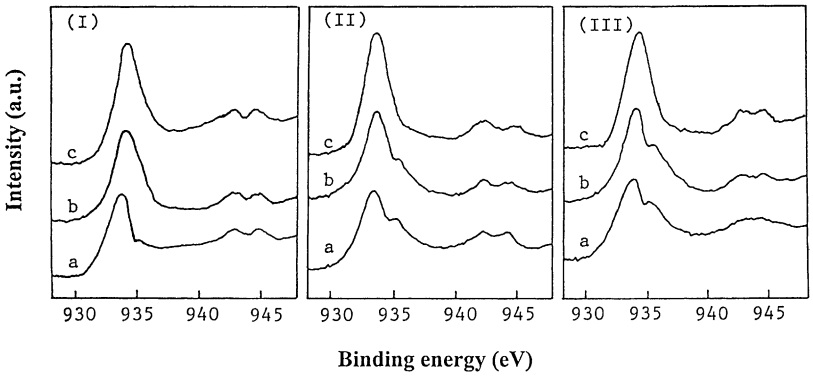

Fig. 4. Cu $2p_{3/2}$ XPS spectra of (I) $ACuO_{1.926}$, (II) $ACuO_{1.901}F_{0.088}$, and (III) $ACuO_{1.950}Cl_{0.036}$ when the samples were treated in He at (a) 520°C, (b) 580°C, and (c) 680°C, respectively.

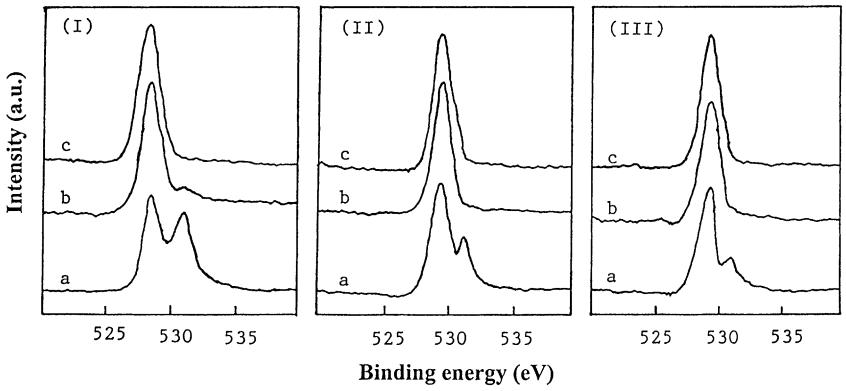

Fig. 5. O 1s XPS spectra of (I) $ACuO_{1.926}$, (II) $ACuO_{1.901}F_{0.088}$, and (III) $ACuO_{1.950}Cl_{0.036}$ when the samples were treated in He at (a) 520°C, (b) 580°C, and (c) 680°C, respectively.

Cu^{3+} ions decreased in intensity with the rise in treatment temperature and disappeared at 680°C, indicating that the concentration of Cu^{3+} ions decreased upon heating in He. The results of the analyses of copper oxidation state support the assignment. The negative results in Cu^{+} analysis and the absence of signals due to Cu^{+} ions in XPS analysis exclude the idea of Cu^{+} presence in these samples. The above results confirm that there are only Cu^{2+} and Cu^{3+} ions in $ACuO_{1.926}$ and $ACuO_{2-\delta}X_{\sigma}$.

Shown in Fig. 5 are the O 1s XPS spectra of the $ACuO_{1.926}$, $ACuO_{1.901}F_{0.088}$, and $ACuO_{1.950}Cl_{0.036}$ samples treated in He at 520, 580, and 680°C, respectively. There are two O 1s peaks at 528.5–529 and 531.0 eV for the three samples treated at 520°C. We assign the signal at lower binding energy to surface lattice oxygen and the one at higher binding energy to adsorbed oxygen species such as O^{-} [23–26]. In view that the O 1s binding energy of OH^{-} falls in the 531–532 eV range, we heated the samples in an oxygen flow at 850°C for 1 h before XPS measurement in order to eliminate the presence of OH^{-}. Furthermore, due to the fact that there was no C 1s signal at ca. 289.5 eV (binding energy), the possible presence of surface carbonates can be discarded. There is only one O 1s peak at ca. 529.5 eV (binding energy) for the $ACuO_{1.901}F_{0.088}$ and $ACuO_{1.950}Cl_{0.036}$ samples treated in He at 580 and 680°C (Fig. 5IIb, IIc, IIIb, and IIIc); it could be assigned to surface lattice oxygen [23–26]. As for the halogen-free $ACuO_{1.926}$ catalyst, with the rise of treatment temperature, the component at ca. 531.0 eV decreased markedly in intensity and disappeared after treatment at 680°C, whereas the intensity of the component at ca. 528.5 eV increased (Fig. 5I). From the O 1s spectra, one can observe that the O 1s binding energy of the lattice oxygen in $ACuO_{1.901}F_{0.088}$ (ca. 529.5 eV) and $ACuO_{1.950}Cl_{0.036}$ (ca. 529.5 eV) was 1.0 eV higher than that (ca. 528.5 eV) in $ACuO_{1.926}$. It might be due to the differences in (i) electronegativity between F and O (which would cause the valence electron density of O^{2-} to decrease and the O 1s binding energy of O^{2-} to rise), and (ii) ionic radii between Cl^{-} and O^{2-} (which would induce the enlargement of the oxide lattice [7–9]). In both cases, the coulombic force between a copper ion and an O^{2-} ion would be weakened. As a result, lattice O^{2-} ions become more active. In other words, the inclusion of F^{-} or Cl^{-} ions in $ACuO_{2-\delta}$ enhances the activity of lattice oxygen. The increase in C_2H_4 selectivity over the halide-doped catalysts (Fig. 2b and c) is a supporting evidence for this viewpoint.

The pioneering work of Ovshinsky et al. [27] initiated a great interest in the investigation of the consequences of anion isomorphism in high-temperature superconductors. Many efforts have been focused on the study of physical properties of these halogenated materials, such as crystal structures, magnetic nature, and superconductivity. It is important to confirm the presence and location of halogen atoms in the crystal lattice. Works on fluorinated $YBa_2Cu_3O_{7-\delta}$ [28–31] manifest that the incorporated halogen atoms occupy

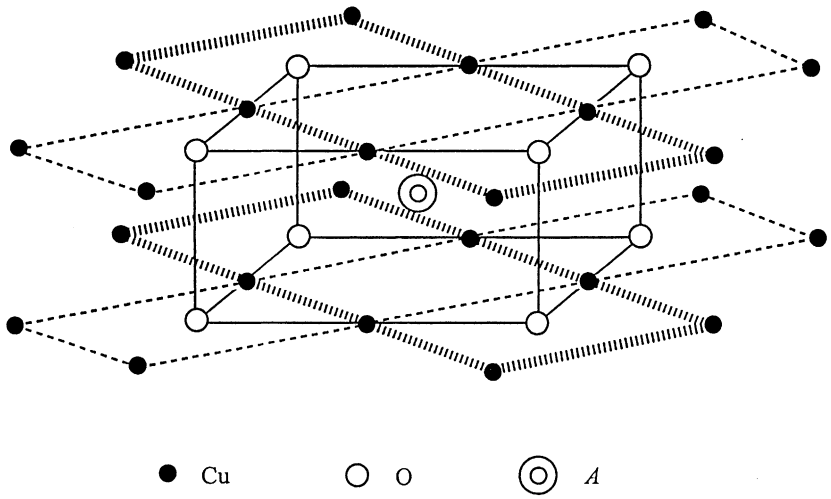

Fig. 6. Schematic crystal structure of $ACuO_{2-\delta}$.

the vacant oxygen positions in the Cu(1) plane where the Cu^{3+} ions are also located [32]. Fig. 6 shows the schematic crystal structure of $ACuO_{2-\delta}$. This unit cell contains two-dimensional CuO_2 sheets that are apparently essential to the high-T_c superconductivity, with the charge carriers arising from the Ca and Sr vacancies. The defect layer could be formulated as $CuO_2/A_{1-x}/CuO_{2-\delta}/A_{1-x}/CuO_2$ ($x > 0.1$) [10]. Compared to O^{2-} (1.40 Å) ions, F^- (1.38 Å) ions are slightly smaller, but Cl^- (1.81 Å) ions are larger in size. Besides occupying the oxygen vacancies, the F^- ions could also dwell at interstitial positions as reported in $Sr_2CuO_2F_{2+\delta}$ [33] or even replace a certain amount of lattice O^{2-} ions. In the first two cases, the Cu^{3+} concentration would increase; in the last case, however, it would cause the Cu^{3+} population to decrease. The fact that the Cu^{3+} content in the F-doped catalyst (Table 1) was lower than that in the Cl-doped catalyst suggests that (i) there was certain extent of O^{2-} replacement by F^- ions, and (ii) the incorporated Cl^- ions could only occupy the oxygen vacancies.

3.3. Active oxygen species

After calcination in an O_2-containing atmosphere, the oxygen vacancies in a catalyst would usually be occupied by dissociatively adsorbed oxygen (O^-). Seiyama et al. [25] determined the exact oxygen composition of $La_{1-x}Sr_xCoO_{3-\delta}$ ($x = 0$–1) before and after the respective desorption peaks, and concluded that a certain amount of Co^{4+} ion was actually induced by the O^- located at oxygen vacancies. In the calcined $ACuO_{2-\delta}$ catalysts, some Cu^{3+} ions were formed due to the occupancy of oxygen vacancies by O^-. Rao [34] reported that there were O^- species settled in the oxygen holes in $YBa_2Cu_3O_{7-\delta}$. The detection of the O 1s signal at ca. 531.0 eV binding energy (Fig. 5) indicates the presence of O^- on/in the $ACuO_{1.926}$ and $ACuO_{2-\delta}X_\sigma$ catalysts. These results demonstrate that there were O^- species accommodated in the oxygen vacancies of the catalysts, driving the Cu^{3+} contents to rise. Compared to $ACuO_{1.926}$, the F- or Cl-doped catalyst showed a weaker signal of O^-, because a lesser amount of oxygen vacancies are available in the halogen-doped catalysts.

Most perovskites (ABO_3) exhibit a characteristic O_2-TPD profile with α- and β-oxygen desorptions. The α-oxygen is accommodated in oxygen vacancies [25,34–36] and is responsible for the complete oxidation of HC; the β-oxygen (i.e. $O^{2-}_{lattice}$) is attributed to the partial reduction of B-site cation and is responsible for the selective oxidation of HC [35,36]. The inclusion of F^- or Cl^- ions in the $ACuO_{2-\delta}$ lattice would result in a decrease in oxygen vacancy population (thus decreasing the amount of α-oxygen) and a rise in Cu^{3+} content (thus increasing β-oxygen desorption). As shown in Table 1, the doping of F^- or Cl^- ions into $ACuO_{2-\delta}$ led to an increase rather than a decrease in

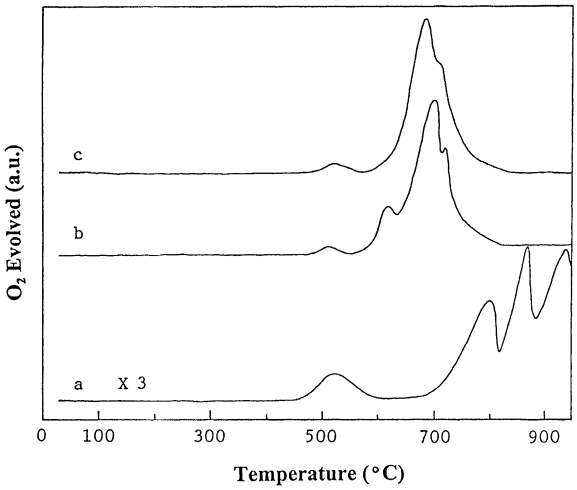

Fig. 7. O_2-TPD profiles of (a) $ACuO_{1.926}$, (b) $ACuO_{1.901}F_{0.088}$, and (c) $ACuO_{1.950}Cl_{0.036}$.

Cu^{3+} content, implying that the F^- or Cl^- ions have occupied a certain amount of oxygen vacancies and/or interstitial sites. Fig. 7 shows the O_2-TPD profiles of $ACuO_{1.926}$ and $ACuO_{2-\delta}X_\sigma$. There were desorptions at 518 ($20.6\,\mu mol\,(g_{cat})^{-1}$), 798, 870, and 938°C for $ACuO_{1.926}$ (Fig. 7a), at 522 ($6.4\,\mu mol\,(g_{cat})^{-1}$), 618, 701, and 721°C for $ACuO_{1.901}F_{0.088}$ (Fig. 7b), and at 528 ($8.2\,\mu mol\,(g_{cat})^{-1}$), 686, and 710°C for $ACuO_{1.950}Cl_{0.036}$ (Fig. 7c). According to the nature of desorbed oxygen species, the peak in the range of 518−528°C could be assigned to α-oxygen, whereas the ones in the range of 618−938°C to β-oxygen. The results of O 1s XPS studies confirm such assignments. The amount of desorbed β-oxygen below 950°C was $56.6\,\mu mol\,(g_{cat})^{-1}$ for $ACuO_{1.926}$, $98.9\,\mu mol\,(g_{cat})^{-1}$ for $ACuO_{1.901}F_{0.088}$, and $86.1\,\mu mol\,(g_{cat})^{-1}$ for $ACuO_{1.950}Cl_{0.036}$. The results of O_2-TPD investigations clearly indicate that with the addition of F^- or Cl^- ions to $ACuO_{2-\delta}$, the content of α-oxygen decreased, whereas that of β-oxygen increased; moreover, the desorption temperature of the β-oxygen was considerably lowered. Therefore, we suggest that the incorporation of F^- or Cl^- ions into the $ACuO_{2-\delta}$ lattice has caused the bulk oxygen vacancy density to decrease (decreasing the amount of α-oxygen) and the lattice oxygen activity to enhance (increasing the amount of β-oxygen), and the complete oxidation reactions were reduced as a result.

Passing oxygen through the catalysts which had just been thermally treated in He (Table 3) would restore the Cu^{3+} contents to the former values (Table 1). The results demonstrate that the oxygen consumed in the ODE reaction could be replenished by the oxygen from the gas phase according to the following sequence:

$$O_2(g) \Leftrightarrow O_2^-(ads) \Leftrightarrow O_2^{2-}(ads) \Leftrightarrow 2O^-_{vacancy}(ads) \Leftrightarrow 2O^{2-}(ads) \Leftrightarrow 2O^{2-}_{lattice}$$

When the treatment temperature was raised from 580 to 720°C, with the removal of $O^{2-}_{lattice}$ from these three catalysts due to the partial reduction of Cu^{3+} ions, the oxygen vacancy density increased, favoring the transformation of gaseous oxygen to $O^{2-}_{lattice}$; as a result, the $O^{2-}_{lattice}$ loss induced by Cu^{3+} reduction is compensated.

Table 4 summarizes the C_2H_6 conversions and C_2H_4 selectivities when the thermally treated $ACuO_{1.926}$, $ACuO_{1.901}F_{0.088}$, and $ACuO_{1.950}Cl_{0.036}$ samples were exposed, respectively, to a C_2H_6 or

Table 4
Catalytic performance of $ACuO_{1.926}$, $ACuO_{1.901}F_{0.088}$, and $ACuO_{1.950}Cl_{0.036}$ in a C_2H_6 or $C_2H_6/O_2/N_2$ pulse after thermal treatments in He, respectively, at 520, 620, 680, and 720°C for 30 min[a]

Catalyst	520°C[b]		620°C[b]		680°C[b]		720°C[b]	
	C_2H_6 conversion (%)	C_2H_4 selectivity (%)	C_2H_6 conversion (%)	C_2H_4 selectivity (%)	C_2H_6 conversion (%)	C_2H_4 selectivity (%)	C_2H_6 conversion (%)	C_2H_4 selectivity (%)
$ACuO_{1.926}$	7.2 (8.6)	31.2 (30.1)	43.3 (45.7)	46.9 (40.8)	60.3 (61.1)	62.4 (53.2)	68.6 (71.4)	78.3 (58.7)
$ACuO_{1.901}F_{0.088}$	6.6 (8.5)	60.1 (61.4)	59.0 (61.4)	71.2 (69.9)	86.8 (84.5)	74.8 (64.1)	91.1 (87.6)	80.9 (62.6)
$ACuO_{1.950}Cl_{0.036}$	10.1 (11.2)	61.7 (62.1)	67.2 (70.1)	72.2 (68.3)	89.9 (88.2)	83.8 (72.6)	93.3 (89.2)	85.4 (76.5)

[a] The values were obtained in a pulse of C_2H_6; values in parentheses were obtained in a pulse of $C_2H_6/O_2/N_2$ (molar ratio = 2/1/3.7).
[b] Temperature for thermal treatment and reactant pulsing.

$C_2H_6/O_2/N_2$ (molar ratio = 2/1/3.7) pulse at various temperatures. In both cases, with a rise in treatment temperature from 520 to 720°C, C_2H_4 selectivity and C_2H_6 conversion increased significantly over the three catalysts. When a C_2H_6 pulse was introduced, respectively, to the three catalysts at 520°C, $ACuO_{1.926}$ showed the highest C_2H_6 conversion but the poorest C_2H_4 selectivity, confirming that the α-oxygen ($O^-_{vacancy}$) tends to induce the complete oxidation of C_2H_6 and C_2H_4. At 580, 620, or 720°C, C_2H_6 conversion and C_2H_4 selectivity recorded in a pulse of C_2H_6 or in a pulse of $C_2H_6/O_2/N_2$ increased significantly over the three catalysts, indicating that the β-oxygen ($O^{2-}_{lattice}$) is accountable for the selective oxidation of C_2H_6 to C_2H_4. Considering the nature and functions of oxygen species on/in the $ACuO_{1.926}$, $ACuO_{1.901}F_{0.088}$, and $ACuO_{1.950}Cl_{0.036}$ catalysts, it is clear that in excessive amount, the $O^-_{vacancy}$ is prone to induce ethane deep oxidation, whereas the $O^{2-}_{lattice}$ is responsible for ethane selective oxidation to ethene.

4. Conclusions

Based on the above results and discussion, we conclude as follows: (i) the halogenated $ACuO_{2-\delta}$ catalysts are tetragonal infinite-layer in structure; (ii) the addition of fluoride or chloride ions to $ACuO_{2-\delta}$ significantly enhanced C_2H_4 selectivity and C_2H_6 conversion; (iii) the inclusion of halide ions in the $ACuO_{2-\delta}$ lattice could promote lattice oxygen activity; (iv) in excessive amount, the mono-oxygen (O^-) species desorbed below 600°C are prone to induce total oxidation, whereas the lattice oxygen species desorbed above 600°C favor selective oxidation of C_2H_6 to C_2H_4; (v) the good and sustainable catalytic behavior of the F- or Cl-doped infinite-layer halo-oxides could be associated with the drop in oxygen vacancy density and the rise in Cu^{3+} population.

Acknowledgements

The work described in this paper was fully supported by a grant from the Research Grants Council of the Hong Kong Special Administration Region, China (project no. HKBU 2015/99P).

References

[1] D. Wang, M.P. Rosynek, J.H. Lunsford, J. Catal. 151 (1995) 155.
[2] W. Ueda, S.W. Lin, I. Tohmoto, Catal. Lett. 44 (1996) 241.
[3] G.H. Yi, T. Hayakawa, A.G. Anderson, K. Suzuki, S. Hamakawa, A.P.E. York, M. Shimizu, K. Takehira, Catal. Lett. 38 (1996) 189.
[4] T. Seiyama, in: L.G. Tejuca, J.L.G. Fierro (Eds.), Properties and Application of Perovskite-Type Oxides, Marcel Dekker, New York, 1993, p. 215.
[5] B. Viswanathan, in: L.G. Tejuca, J.L.G. Fierro (Eds.), Properties and Application of Perovskite-Type Oxides, Marcel Dekker, New York, 1993, p. 271.
[6] H.X. Dai, C.F. Ng, C.T. Au, Catal. Lett. 57 (1999) 115.
[7] H.X. Dai, C.F. Ng, C.T. Au, J. Catal. 189 (2000) 52.
[8] H.X. Dai, C.F. Ng, C.T. Au, J. Catal. 193 (2000) 65.
[9] H.X. Dai, C.F. Ng, C.T. Au, J. Catal. 197 (2001) 251.
[10] M. Azuma, Z. Hiroi, M. Takano, Y. Bando, Y. Takeda, Nature 356 (1992) 775.
[11] U. Asaf, I. Felner, U. Yaron, Physica C 211 (1993) 45.
[12] H.X. Dai, Y.W. Liu, C.F. Ng, C.T. Au, J. Catal. 187 (1999) 59.
[13] C.T. Au, Y.W. Liu, C.F. Ng, J. Catal. 176 (1998) 365.
[14] Z. Hiroi, M. Azuma, M. Takano, Y. Takeda, Physica C 208 (1993) 286.
[15] X.J. Zhou, J.W. Li, F. Wu, J.Q. Li, B. Yin, S.L. Jia, Y.S. Yao, Z.X. Zhao, Physica C 223 (1994) 30.
[16] E.M. Kennedy, N.W. Cant, Appl. Catal. 75 (1991) 321.
[17] C. Shi, M.P. Rosynek, J.H. Lunsford, J. Phys. Chem. 98 (1994) 8371.
[18] Y. Wu, T. Yu, B.S. Dou, C.X. Wang, X.F. Xie, Z.L. Yu, S.R. Fan, Z.R. Fan, L.C. Wang, J. Catal. 120 (1989) 88.
[19] V. Bhat, C.N.R. Rao, J.M. Honig, Solid State Commun. 81 (1992) 751.
[20] T. Tatsuki, S. Adachi, T. Tamura, K. Tanabe, Physica C 303 (1998) 41.
[21] K.S. Kim, J. Electron. Spectrosc. 3 (1974) 217.
[22] J.S. Shin, H. Enomoto, H. Takauchi, Y. Takno, N. Mori, H. Ozaki, Jpn. J. Appl. Phys. 28 (1989) L1365.
[23] G.U. Kulkarni, C.N.R. Rao, M.W. Roberts, J. Phys. Chem. 99 (1995) 3310.
[24] A.F. Carley, M.W. Roberts, A.K. Santra, J. Phys. Chem. B 101 (1997) 9978.
[25] N. Yamazoe, Y. Teraoka, T. Seiyama, Chem. Lett. (1981) 1767.
[26] J.L.G. Fierro, L.G. Tejuca, Appl. Surf. Sci. 27 (1987) 453.
[27] S.R. Ovshinsky, R.T. Young, D.D. Allred, G. Demaggio, G.A. van der Leeden, Phys. Rev. Lett. 58 (1987) 2579.
[28] J.R. LaGraff, E.C. Behrman, J.A.T. Taylor, E.J. Rotella, J.D. Jorgensen, L.Q. Wang, P.G. Mattocks, Phys. Rev. B 39 (1989) 347.
[29] C. Perrin, A. Dinia, O. Pena, M. Sergent, P. Burlet, J. Rossat-Mignod, Solid State Commun. 76 (1990) 401.

[30] M. Mokhtari, C. Perrin, M. Sergent, E. Furet, J.-F. Halet, J.-Y. Saillard, E. Ressouche, P. Burlet, Solid State Commun. 93 (1995) 487.
[31] Yu.A. Ossipyan, O.V. Zharikov, G.Yu. Logvenov, N.S. Sidorov, V.I. Kulakov, I.M. Shmytko, I.K. Bdikin, A.M. Gromov, Physica C 165 (1990) 107.
[32] W.I.F. David, W.T.A. Harrison, J.M.F. Gunn, O. Moze, A.K. Soper, P. Day, J.D. Jorgensen, D.G. Hinks, M.A. Beno, L. Soderholm, D.W. Capone II, I.K. Schuller, C.U. Segre, K. Zhang, J.D. Grace, Nature 327 (1987) 310.
[33] M. Al-Mamouri, P.P. Edwards, C. Greaves, M. Slaski, Nature 369 (1994) 382.
[34] C.N.R. Rao, in: C.N.R. Rao (Ed.), Chemistry of Oxide Superconductivity, Blackwell, Oxford, 1988, p. 1.
[35] A. Bielañski, J. Haber, Oxygen in Catalysis, Marcel Dekker, New York, 1991.
[36] J. Haber, in: J.P. Bonnelle, B. Delmon, E. Derouane (Eds.), Surface Properties and Catalysis by Non-Metals, Reidel, Dordrecht, 1983.